

## Adsorption-controlled growth of BiMnO<sub>3</sub> films by molecular-beam epitaxy

J. H. Lee, X. Ke, R. Misra, J. F. Ihlefeld, X. S. Xu, Z. G. Mei, T. Heeg, M. Roeckerath, J. Schubert, Z. K. Liu, J. L. Musfeldt, P. Schiffer, and D. G. Schlom

Citation: *Applied Physics Letters* **96**, 262905 (2010); doi: 10.1063/1.3457786

View online: <http://dx.doi.org/10.1063/1.3457786>

View Table of Contents: <http://scitation.aip.org/content/aip/journal/apl/96/26?ver=pdfcov>

Published by the *AIP Publishing*

---

### Articles you may be interested in

[Adsorption-controlled growth of BiVO<sub>4</sub> by molecular-beam epitaxy](#)

*APL Mat.* **1**, 042112 (2013); 10.1063/1.4824041

[The adsorption-controlled growth of LuFe<sub>2</sub>O<sub>4</sub> by molecular-beam epitaxy](#)

*Appl. Phys. Lett.* **101**, 132907 (2012); 10.1063/1.4755765

[Adsorption-controlled growth of EuO by molecular-beam epitaxy](#)

*Appl. Phys. Lett.* **93**, 102105 (2008); 10.1063/1.2973180

[Optical band gap of Bi Fe O<sub>3</sub> grown by molecular-beam epitaxy](#)

*Appl. Phys. Lett.* **92**, 142908 (2008); 10.1063/1.2901160

[Adsorption-controlled molecular-beam epitaxial growth of Bi Fe O<sub>3</sub>](#)

*Appl. Phys. Lett.* **91**, 071922 (2007); 10.1063/1.2767771

---

An advertisement for Oxford Instruments Atomic Force Microscopy (AFM) systems. The background is a dark blue gradient. On the left, there is a black mobile phone and a beige desktop computer with a monitor and keyboard. In the center, there is a white AFM instrument. Text on the left side reads: 'You don't still use this cell phone' and 'or this computer'. Text in the center reads: 'Why are you still using an AFM designed in the 80's?'. On the right side, text reads: 'It is time to upgrade your AFM', 'Minimum \$20,000 trade-in discount for purchases before August 31st', and 'Asylum Research is today's technology leader in AFM'. At the bottom right, there is the Oxford Instruments logo and the tagline 'The Business of Science®'. The email address 'dropmyoldAFM@oxinst.com' is also present.

# Adsorption-controlled growth of BiMnO<sub>3</sub> films by molecular-beam epitaxy

J. H. Lee,<sup>1,2</sup> X. Ke,<sup>3</sup> R. Misra,<sup>3</sup> J. F. Ihlefeld,<sup>2</sup> X. S. Xu,<sup>4</sup> Z. G. Mei,<sup>2</sup> T. Heeg,<sup>1</sup> M. Roeckerath,<sup>5</sup> J. Schubert,<sup>5</sup> Z. K. Liu,<sup>2</sup> J. L. Musfeldt,<sup>4</sup> P. Schiffer,<sup>3</sup> and D. G. Schlom<sup>1,a)</sup>

<sup>1</sup>Department of Materials Science and Engineering, Cornell University, Ithaca, New York 14853, USA

<sup>2</sup>Department of Materials Science and Engineering, Pennsylvania State University, University Park, Pennsylvania 16802, USA

<sup>3</sup>Department of Physics, Pennsylvania State University, University Park, Pennsylvania 16802, USA

<sup>4</sup>Department of Chemistry, University of Tennessee, Knoxville, Tennessee 37996, USA

<sup>5</sup>Institute of Bio- and Nano-Systems (IBNI-IT), JARA-Fundamentals of Future Information Technology, Research Centre Jülich, D-52425 Jülich, Germany

(Received 20 February 2010; accepted 4 June 2010; published online 2 July 2010)

We have developed the means to grow BiMnO<sub>3</sub> thin films with unparalleled structural perfection by reactive molecular-beam epitaxy and determined its band gap. Film growth occurs in an adsorption-controlled growth regime. Within this growth window bounded by oxygen pressure and substrate temperature at a fixed bismuth overpressure, single-phase films of the metastable perovskite BiMnO<sub>3</sub> may be grown by epitaxial stabilization. X-ray diffraction reveals phase-pure and epitaxial films with  $\omega$  rocking curve full width at half maximum values as narrow as 11 arc sec (0.003°). Optical absorption measurements reveal that BiMnO<sub>3</sub> has a direct band gap of  $1.1 \pm 0.1$  eV. © 2010 American Institute of Physics. [doi:10.1063/1.3457786]

Multiferroic materials are being studied for their rich properties, fascinating physics, and application potential.<sup>1</sup> Bismuth manganite, BiMnO<sub>3</sub>, is a well-known, but controversial multiferroic. Early first-principles calculations suggested that BiMnO<sub>3</sub> might be simultaneously ferroelectric and ferromagnetic, arising from bismuth 6s lone pairs and magnetic ordering of manganese.<sup>2</sup> Subsequent experiments confirmed multiferroism in thin films.<sup>3–5</sup> The prediction of its ferroelectricity was based on the reported noncentrosymmetric C2 space group of BiMnO<sub>3</sub>.<sup>6–8</sup> Recent calculations and experiments, however, find that BiMnO<sub>3</sub> belongs to the centrosymmetric C2/c space group and therefore stoichiometric BiMnO<sub>3</sub> may not be a multiferroic at all.<sup>9,10</sup>

To better establish the properties of BiMnO<sub>3</sub>, we have grown films of it by reactive molecular-beam epitaxy (MBE) using adsorption-controlled growth conditions. Adsorption-controlled growth conditions are the standard way of growing phase-pure compound semiconductors;<sup>11</sup> it has also been applied to the growth of ferroelectric oxide thin films.<sup>12,13</sup> In this letter, we first describe the adsorption-controlled growth of single phase BiMnO<sub>3</sub> films by controlling bismuth overpressure, substrate temperature, and oxidant partial pressure. The ferromagnetic properties and optical absorption spectrum of the grown films are then reported.

The pressure-temperature region for the adsorption-controlled growth of BiMnO<sub>3</sub> was calculated using the CALPHAD approach.<sup>14</sup> It was empirically established using *in situ* reflection high-energy electron diffraction (RHEED) and confirmed by *ex situ* four circle x-ray diffraction (XRD). Figure 1 shows a calculated Ellingham diagram representing the phase stability regions of (I) BiMnO<sub>3</sub>+Mn<sub>2</sub>O<sub>3</sub>, (II) BiMnO<sub>3</sub>, and (III) BiMnO<sub>3</sub>+Bi<sub>2</sub>O<sub>2.5</sub> as a function of substrate temperature and O<sub>2</sub> overpressure. The boundaries between regions I, II, and III were calculated with the Gibbs free energy functions of the gas phase containing various

bismuth and Bi–O species and the stable and metastable manganese and bismuth oxides.<sup>15</sup> Unfortunately there is no Gibbs free energy of formation reported for BiMnO<sub>3</sub> or Bi<sub>2</sub>O<sub>2.5</sub>. First-principles calculations, using the generalized gradient approximation (GGA) and GGA plus Hubbard *U* (GGA+*U*) method, predicted the enthalpy of formation of BiMnO<sub>3</sub> to be between +400 J/mol and +4000 J/mol of BiMnO<sub>3</sub> with respect to Bi<sub>2</sub>O<sub>3</sub> and Mn<sub>2</sub>O<sub>3</sub>, respectively.<sup>16</sup> Since there is no detailed crystal structure of Bi<sub>2</sub>O<sub>2.5</sub> available for first-principles calculations, we assume its enthalpy of formation to be +100 J/mol or +4500 J/mol with respect to bismuth and Bi<sub>2</sub>O<sub>3</sub>, as assumed in Ref. 13. The phase stability region was calculated using THERMOCALC<sup>17</sup> with the partial pressure of bismuth fixed at  $2.6 \times 10^{-10}$  atm, which

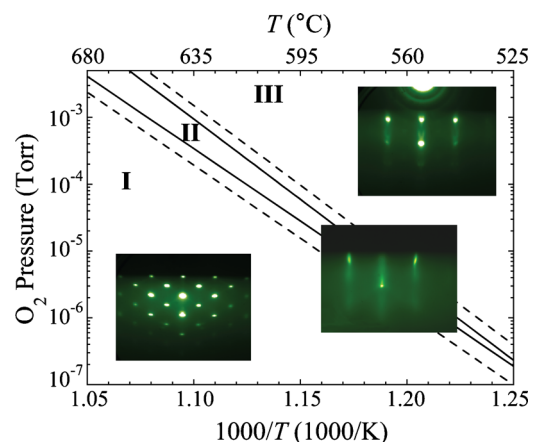


FIG. 1. (Color online) Calculated Ellingham diagram and RHEED patterns collected along the [110] azimuth of SrTiO<sub>3</sub> during the deposition of BiMnO<sub>3</sub> at different temperatures and oxygen partial pressures. Solid lines represent phase boundaries using +4000 J/mol and +100 J/mol formula unit Gibbs free energies for BiMnO<sub>3</sub> and Bi<sub>2</sub>O<sub>2.5</sub>, respectively, specifying the narrowest growth window possible. Dashed lines are for +400 J/mol and +4500 J/mol formula unit, indicating the approximate uncertainty in width of the growth window. Phase stability between Bi<sub>x</sub>O<sub>y</sub> gases and BiMnO<sub>3</sub>+Mn<sub>2</sub>O<sub>3</sub>, BiMnO<sub>3</sub>, and BiMnO<sub>3</sub>+Bi<sub>2</sub>O<sub>2.5</sub> condensed phases is represented by regions I, II, and III, respectively.

<sup>a)</sup>Electronic mail: schlom@cornell.edu.

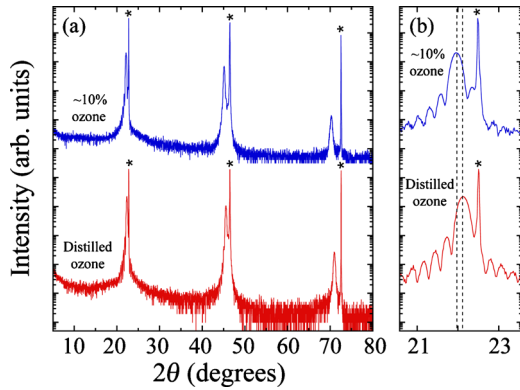


FIG. 2. (Color online) (a)  $\theta$ - $2\theta$  XRD scans of BiMnO<sub>3</sub> films grown on (001) SrTiO<sub>3</sub> at an oxidant background pressure of  $1 \times 10^{-6}$  Torr and the 3:1 Bi:Mn flux ratio stated above. The difference was that one film was grown in  $\sim 10\%$  ozone directly out of an ozone generator at  $T_{\text{sub}} = 590$  °C whereas the other was grown using distilled ozone ( $\sim 80\%$  ozone) at  $T_{\text{sub}} = 630$  °C. Substrate peaks are marked with an asterisk. (b) A close-up of the 001 peak, showing a clear difference in the out-of-plane lattice constant.

corresponds to the pressure at the plane of the substrate for an incident bismuth flux of  $5.5 \times 10^{13}$  atom/(cm<sup>2</sup> s).<sup>18</sup>

BiMnO<sub>3</sub> thin films were deposited on buffered-HF treated (001) SrTiO<sub>3</sub> (Ref. 19) and (110) DyScO<sub>3</sub> substrates in a similar manner to previous adsorption-controlled oxides by MBE.<sup>12,13</sup> The volatile bismuth and oxygen components were supplied continuously and the nonvolatile component (manganese) was supplied in doses corresponding to individual (MnO<sub>2</sub>) monolayers making up the BiO–MnO<sub>2</sub>–BiO–MnO<sub>2</sub>–... stacking sequence along the [001] pseudocubic growth direction of the BiMnO<sub>3</sub> perovskite structure. Due to the narrow growth window for phase-pure BiMnO<sub>3</sub> growth (region II in Fig. 1), the substrate temperature was monitored *in situ* by measuring the absorption edge of the SrTiO<sub>3</sub> substrate.<sup>20</sup> The thermodynamic predictions were verified by investigating a horizontal slice through Fig. 1 at constant bismuth [bismuth flux =  $5.5 \times 10^{13}$  Bi/(cm<sup>2</sup> s)] and oxygen (O<sub>2</sub> +  $\sim 10\%$  O<sub>3</sub> background pressure =  $1 \times 10^{-6}$  Torr) overpressure during the deposition of Bi–Mn–O over a temperature range of 580–690 °C and a fixed Bi:Mn flux ratio of 3:1. The *in situ* RHEED patterns collected along the  $\langle 110 \rangle$  azimuthal direction of (001)-oriented SrTiO<sub>3</sub> delineating the three regions are superimposed in Fig. 1. Above 650 °C (region I), RHEED spots are observed and can be indexed to diffraction from (101)-oriented Mn<sub>3</sub>O<sub>4</sub>. The presence of this phase was verified by *ex situ* XRD. Between 610 and 640 °C (region II), phase-pure BiMnO<sub>3</sub> can be grown. Below 610 °C (region III), additional spots form, which can be indexed by *ex situ* XRD as (001)- and (110)-oriented Bi<sub>2</sub>O<sub>2.5</sub>. The occurrence of these spots corresponds to the phase boundary separating region II and III. A change in bismuth flux or oxygen activity results in a shift in the growth window of single-phase BiMnO<sub>3</sub> (region II in Fig. 1). The calculated O<sub>2</sub> overpressures compare well with what is expected given the enhanced activity of O<sub>3</sub> and our directed gas inlet that locally increases the oxygen pressure at the substrate surface.<sup>18</sup>

The structure of two 29 nm thick BiMnO<sub>3</sub> films deposited on (001) SrTiO<sub>3</sub> was characterized. Both films were grown under adsorption-controlled conditions (region II in Fig. 1).  $\theta$ - $2\theta$  XRD scans of both films in Fig. 2(a) reveal them to be phase-pure and epitaxial. The full width at half

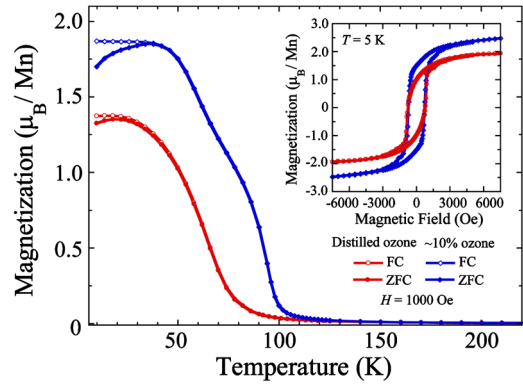


FIG. 3. (Color online) Field-cooled and zero field-cooled magnetization of the same BiMnO<sub>3</sub> films as Fig. 2 grown using  $\sim 10\%$  ozone and distilled ozone. (Inset) Magnetic hysteresis of these films at 5 K.

maximum (FWHM) of the  $\omega$  rocking curve of the pseudocubic 002 film peaks are equal to 80 arc sec ( $0.02^\circ$ ) and 36 arc sec ( $0.01^\circ$ ), which are the same as the underlying SrTiO<sub>3</sub> substrates. Both films show clear thickness fringes [Fig. 2(b)], corresponding to a film thickness of  $29 \pm 2$  nm. The out-of-plane lattice constant was calculated to be  $4.01 \pm 0.01$  Å for the BiMnO<sub>3</sub> films grown in  $\sim 10\%$  ozone and  $3.98 \pm 0.01$  Å for the film grown in distilled ozone. The extended out-of-plane lattice constants result from the lattice mismatch between the SrTiO<sub>3</sub> substrate ( $a = 3.905$  Å) and the BiMnO<sub>3</sub> film ( $a_{\text{pseudocubic}} = 3.95$  Å).<sup>10</sup> The  $\sim 0.03$  Å difference in out-of-lattice constants between the two samples is a result of the different oxidating atmosphere during growth. The films grown in  $\sim 10\%$  ozone show a longer lattice constant than the films grown in distilled ozone. Rutherford backscattering spectrometry confirms that the ratio of Bi:Mn of these films is 1:1 within the 5% experimental error of the measurements.

Magnetic measurements on the same two BiMnO<sub>3</sub> films are shown in Fig. 3. Both films exhibit clear ferromagnetic hysteresis loops. The oxygen-rich films tend to show lower  $T_C$  and saturation magnetization than the oxygen-stoichiometric films. BiMnO<sub>3</sub> films grown in  $\sim 10\%$  ozone showed a ferromagnetic transition at  $\sim 105$  K, which is close to  $T_C$  of bulk BiMnO<sub>3</sub>, and a magnetization value of  $2.5 \mu_B/\text{Mn}$  at 5 K. In contrast, films grown in distilled ozone showed a  $T_C$  at  $\sim 95$  K and a magnetization value of  $1.9 \mu_B/\text{Mn}$  at 5 K. A depression of  $T_C$  has been reported in films grown by pulsed-laser deposition.<sup>3,21</sup> We attribute it to oxygen stoichiometry since the Bi:Mn ratio was observed not to influence the transition temperature. Measurements on bulk BiMnO<sub>3+x</sub> ( $0 < x < 0.16$ ) samples also observed this depression of  $T_C$  and magnetization in samples with higher oxygen content.<sup>10</sup>

The optical spectra of BiMnO<sub>3</sub> films were measured in transmittance using a Perkin–Elmer Lambda-900 spectrometer (3000–190 nm and 0.41–6.53 eV) with bare substrates as references. The film on DyScO<sub>3</sub> had a rocking curve FWHM of 11 arc sec ( $0.003^\circ$ ), comparable to the underlying DyScO<sub>3</sub> substrate and over  $100\times$  narrower than any reported BiMnO<sub>3</sub> film.<sup>3–5</sup> Absorption was calculated as  $\alpha(E) = -(1/d)\ln[T(E)]$ , where  $d$  is the film thickness,  $T$  is the measured transmittance, and  $E$  is the energy of the light.

Figure 4 displays the absorption spectrum of BiMnO<sub>3</sub> at 300 and 4 K. The onset of optical absorption in BiMnO<sub>3</sub> is  $\sim 0.75$  eV (1650 nm),<sup>22</sup> much lower than the  $\sim 2.2$  eV

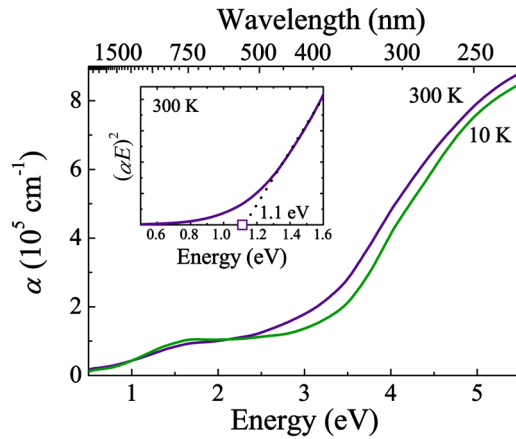


FIG. 4. (Color online) Optical absorption spectrum of 33 nm thick BiMnO<sub>3</sub> films grown on (001) SrTiO<sub>3</sub> and (110) DyScO<sub>3</sub> at  $T_{\text{sub}}=640$  °C in a background pressure of  $1 \times 10^{-6}$  Torr of distilled ozone were combined to create a composite absorption curve and were identical in the overlap regime. (Inset) Charge gap extraction from 300 K absorption.

(560 nm) onset in BiFeO<sub>3</sub> thin films.<sup>13,23,24</sup> Peaks occur at  $\sim 1.6$  eV (780 nm) and  $\sim 5.5$  eV (230 nm), with a broad shoulder near 4 eV. The near-infrared feature in perovskite manganites has been studied extensively.<sup>25–28</sup> Relevant predictions from first-principles electronic structure calculations for BiMnO<sub>3</sub> include strong Mn–O hybridization, a stereochemically active Bi lone pair that mixes Bi and O states, and insulating behavior in calculations that employ strong exchange correlation.<sup>29,29,30</sup> Several very different assignments might reasonably account for the 1.6 eV near infrared excitation in BiMnO<sub>3</sub>: (i) on-site excitations between crystal field split 3d levels, (ii) charge transfer excitations involving strongly hybridized Mn<sup>3+</sup> and oxygen states, or (iii) transitions between localized Hubbard bands. Based upon comparison with electronic structure calculations,<sup>29,23,30</sup> the experimental spectrum of chemically similar materials with Mn<sup>3+</sup> centers in locally distorted octahedral environments such as LaMnO<sub>3</sub>,<sup>25–28</sup> and the overall intensity ( $\alpha \sim 1.05 \times 10^{-5}$  cm<sup>-1</sup>), we assign the near infrared peak at  $\sim 1.6$  eV to charge transfer excitations between mixed O 2p and Mn 3d states. The limited temperature dependence of the 1.6 eV structure supports this assignment. A plot of  $(\alpha E)^2$  versus energy (inset, Fig. 4) places the 300 K charge gap in BiMnO<sub>3</sub> at  $\sim 1.1 \pm 0.1$  eV.<sup>22</sup> Our fitting indicates that BiMnO<sub>3</sub> has a direct band gap. The relatively small direct band gap of BiMnO<sub>3</sub> could be relevant to ferroelectric solar cell applications, e.g., creating a solid solution with BiFeO<sub>3</sub> with  $E_g = 2.7$  eV (Refs. 13, 23, and 24) could result in a band gap ideally matched to the solar spectrum.

According to electronic structure calculations,<sup>30</sup> the charge excitations are predicted to be strongly spin polarized. The gap is determined by majority carriers, and minority states are involved only above 3 eV. Higher energy excitations [above 3.7 eV (330 nm)] are assigned as O 2p  $\rightarrow$  Mn 3d charge transfer, with some mixing of Bi 6p levels above 3 eV. The aforementioned electronic excitations sharpen and blueshift slightly with decreasing temperature (Fig. 4). We find no obvious anomalies at the 105 K Curie temperature within our sensitivity, indicative of modest charge-spin interactions.

We gratefully acknowledge the financial support from the National Science Foundation through Grant No. DMR-0507146 and the MRSEC program (Grant No. DMR-0820404) and from the U.S. DOE through Grant No. DE-FG02-01-ER45885(UT).

- <sup>1</sup>W. Eerenstein, N. D. Mathur, and J. F. Scott, *Nature (London)* **442**, 759 (2006).
- <sup>2</sup>N. A. Hill and K. M. Rabe, *Phys. Rev. B* **59**, 8759 (1999).
- <sup>3</sup>A. Moreira dos Santos, A. K. Cheetham, W. Tian, X. Pan, Y. Jia, N. Murphy, J. Lettieri, and D. G. Schlom, *Appl. Phys. Lett.* **84**, 91 (2004).
- <sup>4</sup>A. Sharan, J. Lettieri, Y. Jia, W. Tian, X. Pan, D. G. Schlom, and V. Gopalan, *Phys. Rev. B* **69**, 214109 (2004).
- <sup>5</sup>J. Y. Son and Y.-H. Shin, *Appl. Phys. Lett.* **93**, 062902 (2008).
- <sup>6</sup>T. Atou, H. Chiba, K. Ohoyama, Y. Yamaguchi, and Y. Syono, *J. Solid State Chem.* **145**, 639 (1999).
- <sup>7</sup>A. Moreira dos Santos, A. K. Cheetham, T. Atou, Y. Syono, Y. Yamaguchi, K. Ohoyama, H. Chiba, and C. N. R. Rao, *Phys. Rev. B* **66**, 064425 (2002).
- <sup>8</sup>K. Kodama, S. Iikubo, S. Shamoto, A. A. Belik, and E. Takayama-Muromachi, *J. Phys. Soc. Jpn.* **76**, 124605 (2007).
- <sup>9</sup>P. Baettig, R. Seshadri, and N. A. Spaldin, *J. Am. Chem. Soc.* **129**, 9854 (2007).
- <sup>10</sup>A. A. Belik, T. Kolodiazny, K. Kosuda, and E. Takayama-Muromachi, *J. Mater. Chem.* **19**, 1593 (2009).
- <sup>11</sup>J. Y. Tsao, *Materials Fundamentals of Molecular Beam Epitaxy* (Academic, Boston, 1993).
- <sup>12</sup>D. G. Schlom, J. H. Haeni, J. Lettieri, C. D. Theis, W. Tian, J. C. Jiang, and X. Q. Pan, *Mater. Sci. Eng., B* **87**, 282 (2001).
- <sup>13</sup>J. F. Ihlefeld, N. J. Podraza, Z. K. Liu, R. C. Rai, X. Xu, T. Heeg, Y. B. Chen, J. Li, R. W. Collins, J. L. Musfeldt, X. Q. Pan, J. Schubert, R. Ramesh, and D. G. Schlom, *Appl. Phys. Lett.* **92**, 142908 (2008).
- <sup>14</sup>L. Kaufman, CALPHAD: Comput. Coupling Phase Diagrams Thermochem. **25**, 141 (2001).
- <sup>15</sup>Scientific Group Thermodata Europe, in *Thermodynamic Properties of Inorganic Materials*, Landolt-Börnstein, New Series, Group IV Vol. 19, edited by Lehrstuhl für Theoretische Hüttenkunde (Springer, Berlin, 1999).
- <sup>16</sup>Z. G. Mei, S. Shang, Y. Wang, D. G. Schlom, and Z. K. Liu (unpublished).
- <sup>17</sup>J. O. Andersson, T. Helander, L. H. Hoglund, P. F. Shi, and B. Sundman, CALPHAD: Comput. Coupling Phase Diagrams Thermochem. **26**, 273 (2002).
- <sup>18</sup>D. G. Schlom and J. S. J. Harris, in *Molecular Beam Epitaxy: Applications to Key Materials*, edited by R. F. C. Farrow (Noyes, Park Ridge, NJ, 1995), pp. 505–622.
- <sup>19</sup>G. Koster, B. L. Kropman, G. Rijnders, D. H. A. Blank, and H. Rogalla, *Appl. Phys. Lett.* **73**, 2920 (1998).
- <sup>20</sup>kSA BandiT, k-Space Associates, Ann Arbor, MI.
- <sup>21</sup>S. Fujino, M. Murakami, S.-H. Lim, L. G. Salamanca-Riba, M. Wuttig, and I. Takeuchi, *J. Appl. Phys.* **101**, 013903 (2007).
- <sup>22</sup>The  $\pm 0.1$  eV error bars on the gap and the background absorption in BiMnO<sub>3</sub> come from the small film thickness (and the associated challenges in growing BiMnO<sub>3</sub> films with thicknesses >33 nm). Fortunately, they do not obscure the most important physics.
- <sup>23</sup>S. R. Basu, L. W. Martin, Y. H. Chu, M. Gajek, R. Ramesh, R. C. Rai, X. Xu, and J. L. Musfeldt, *Appl. Phys. Lett.* **92**, 091905 (2008).
- <sup>24</sup>A. Kumar, R. C. Rai, N. J. Podraza, S. Denev, M. Ramirez, Y.-H. Chu, L. W. Martin, J. Ihlefeld, T. Heeg, J. Schubert, D. G. Schlom, J. Orenstein, R. Ramesh, R. W. Collins, J. L. Musfeldt, and V. Gopalan, *Appl. Phys. Lett.* **92**, 121915 (2008).
- <sup>25</sup>K. Tobe, T. Kimura, Y. Okimoto, and Y. Tokura, *Phys. Rev. B* **64**, 184421 (2001).
- <sup>26</sup>M. A. Quijada, J. R. Simpson, L. Vasiliu-Doloc, J. W. Lynn, H. D. Drew, Y. M. Mukocskii, and S. G. Karabashev, *Phys. Rev. B* **64**, 224426 (2001).
- <sup>27</sup>M. W. Kim, P. Murugavel, S. Parashar, J. S. Lee, and T. W. Noh, *New J. Phys.* **6**, 156 (2004).
- <sup>28</sup>N. N. Kovaleva, A. V. Boris, C. Bernhard, A. Kulakov, A. Pimenov, A. M. Balbashov, G. Khaliullin, and B. Keimer, *Phys. Rev. Lett.* **93**, 147204 (2004).
- <sup>29</sup>R. Seshadri and N. A. Hill, *Chem. Mater.* **13**, 2892 (2001).
- <sup>30</sup>P. Baettig, R. Seshadri, and N. A. Spaldin, private communication (September 26, 2008).